

Meeting-report

The Behavior of Ti-15Zr-5Nb in Very Aggressive Environments

Julia Mirza-Rosca^{1,2}, Iosif Hulka³, Ioan Aron⁴, and Jenifer Vaswani-Reboso⁵

¹Mechanical Engineering Department, University of Las Palmas de Gran Canaria, Las Palmas de Gran Canaria, Spain

²Materials Engineering and Welding Department, Transylvania University of Brasov, Brasov, Romania

³Research Institute for Renewable Energy, Politehnica University Timisoara, Timisoara, Romania

⁴Law Department, Faculty of Law, Transylvania University of Brasov, Brasov, Romania

⁵Processes Engineering Department, University of Las Palmas de Gran Canaria, Las Palmas de Gran Canaria, Spain

*Correspondence: julia.mirza@ulpgc.es

Introduction

In the field of biomedical implants, metals are utilized for a variety of body parts. Corrosion products can be a source of local bodily pain, infections, swelling, and failure of implants [1]. The in-vivo environment, which consists of body fluid, is a very aggressive environment toward the metallic surface. When it comes to choosing biomaterials, biocompatibility is an extremely important factor to consider. Stainless steel 316, titanium and its alloys, and cobalt-chromium alloys were the primary components in the development of the most widely used corrosion-resistant metallic biomaterials.

Ti alloys are the materials that have the highest corrosion resistance, specific strength, and biocompatibility among these materials. The protection against corrosion that is provided by passive film is an essential component in the corrosion process of titanium alloys [2, 3]. Ti-Zr-Nb ternary alloys were investigated as potential candidates for use as biomaterials due to the fact that they possess the benefit of a composition that is fully composed of non-toxic elements and possesses an exceptional resistance to corrosion [4, 5].

Using electrochemical methods, the purpose of our work is to investigate the corrosion behavior of Ti-15Zr-5Nb alloy in comparison to titanium in a very aggressive environment.

Experimental

The alloy examined in this study was produced in its as-cast state utilizing a double vacuum electronic flow melting FiveCell oven from France. Cylindrical samples were cut from the resultant ingot to facilitate microstructural and electrochemical analysis.

An Olympus PME 3-ADL metallographic microscope, manufactured by Olympus in Tokyo, Japan, was used to conduct optical metallographic investigations. The microstructure of the alloy was examined using a scanning electron microscope (FE-SEM Zeiss Sigma 300 VP, Carl Zeiss, Jena, Germany) equipped with an energy dispersive X-ray spectrometer (EDS).

The specimens were sectioned and encapsulated in a carbon-based resin to prevent damage to the edges during the processes of grinding and polishing. Subsequently, a copper wire was affixed to the sample to ensure proper electrical connection between the working electrode and the potentiostat for the electrochemical measurements.

The electrochemical behavior of Ti-15Zr-5Nb and cpTi was analyzed using Cyclic Voltammetry (CV), linear polarization (LP), and Electrochemical Impedance Spectroscopy (EIS). The electrochemical experiments were conducted at a temperature of around 22°C, utilizing a standard electrochemical glass cell containing 350 ml of HCl solution with a pH = 2.5. The working electrode's potential was determined relative to a saturated calomel electrode (SCE) immersed in potassium chloride (KCl) solution. A platinum gauze served as the counter electrode.

Results and discussion

The scanning electron microscope (SEM) micrographs in Fig.1 (labeled a and b) displayed the acicular microstructure and grain boundary. The material's microstructure comprised of needle-shaped α within a modified β matrix [6]. In addition, it was observed that there were continuous grain boundaries with a high concentration of the α phase, which were occasionally accompanied by the β phase adjacent to it.

Energy Dispersive X-ray spectroscopy (EDS) was employed to analyze the chemical composition of the sample, as depicted in Fig.1 (labeled c,d and e). It is evident that Area A, which corresponds to the α phase, contains a high concentration of titanium, whereas Area B, corresponding to the β phase, has a reduced titanium content and is enriched with alloying elements. This is characteristic of the β phase, which exhibits a greater affinity for Nb and Zr, serving as phase stabilizing elements in the alloy.

Electrochemical Impedance Spectroscopy (EIS) is an effective analytical method employed to study the electrochemical processes occurring at the contact between a material and an electrolyte solution. Electrochemical impedance spectroscopy (EIS) is employed in the analysis of corrosion to gain insight into the degradation of metals and alloys caused by electrochemical reactions.

The Nyquist plot, depicted in Fig.2a, is a crucial graphical representation used in the investigation of Electrochemical Impedance Spectroscopy (EIS). By displaying impedance data in the complex plane, it offers valuable insights into the electrochemical characteristics of a system, as Bode plots (see Fig.3) [7].

The semi-circle's diameter represents the resistance associated with the transmission of charge in the system. A bigger diameter indicates increased transfer resistance due to the presence of a protective layer on the surface. The semi-circle's center often lies close to the actual axis, suggesting that the solution resistance (R_s) is negligible.

Upon examining the contours of the impedance spectra, the obtained experimental data will be converted into a corresponding electrical model (see Fig.4.) An analogous circuit refers to a group of passive components, such as resistors, capacitors, inductors, and other types of distributed impedance, that exhibit behavior similar to corrosion in the specific frequency range being studied.

The Constant Phase Element (CPE) developed by Boukamp [1, 8] offers improved outcomes. It is a variable component in electrical equivalent circuits that can identify a wide range of electrochemical behaviors in impedance spectroscopy, specifically those involving non-ideal capacitive, inductive, and resistive properties. The value "n" enables the continual change of the phase angle, hence facilitating a more precise representation of complex electrochemical systems. The real system's reaction is more closely aligned with the ideal due to the proximity of the value of n to unity and the increased uniformity of the surface. Consequently, when n is equal to 0, the CPE element may be described as a basic resistance. On the other hand, when n is equal to 1, the CPE element can be characterized as a capacitor with a capacitance of Y^0 .

The EIS experimental data was fitted using the circuit depicted in Fig.4, incorporating the following components:

- the term "Solution Resistance (R_{sol})" refers to the resistance that arises from the electrolyte solution through which the current passes;
- CPE_1 refers to the porous exterior passive layer.
- R_1 represents the resistance associated with the external porous layer.
- CPE_2 relates to the compact interior passive layer.
- R_2 denotes the polarization resistance of the alloy.

From the results of the fitting it was observed that the resistance against corrosion of the Ti-15Zr-5Nb in an aggressive environment is 4 times less compared with that of cpTi.

Conclusions

Although Ti-15Zr-5Nb has shown excellent corrosion resistance in simulated oral environments and Ringer's solutions compared to cp-Ti as reported by other researchers, this study demonstrates that the Ti-15Zr-5Nb alloy has lower corrosion resistance in aggressive environments compared to cp-Ti. This is attributed to the presence of soluble Zr^{4+} ions on the surface of the alloy, which form in highly acidic environments.

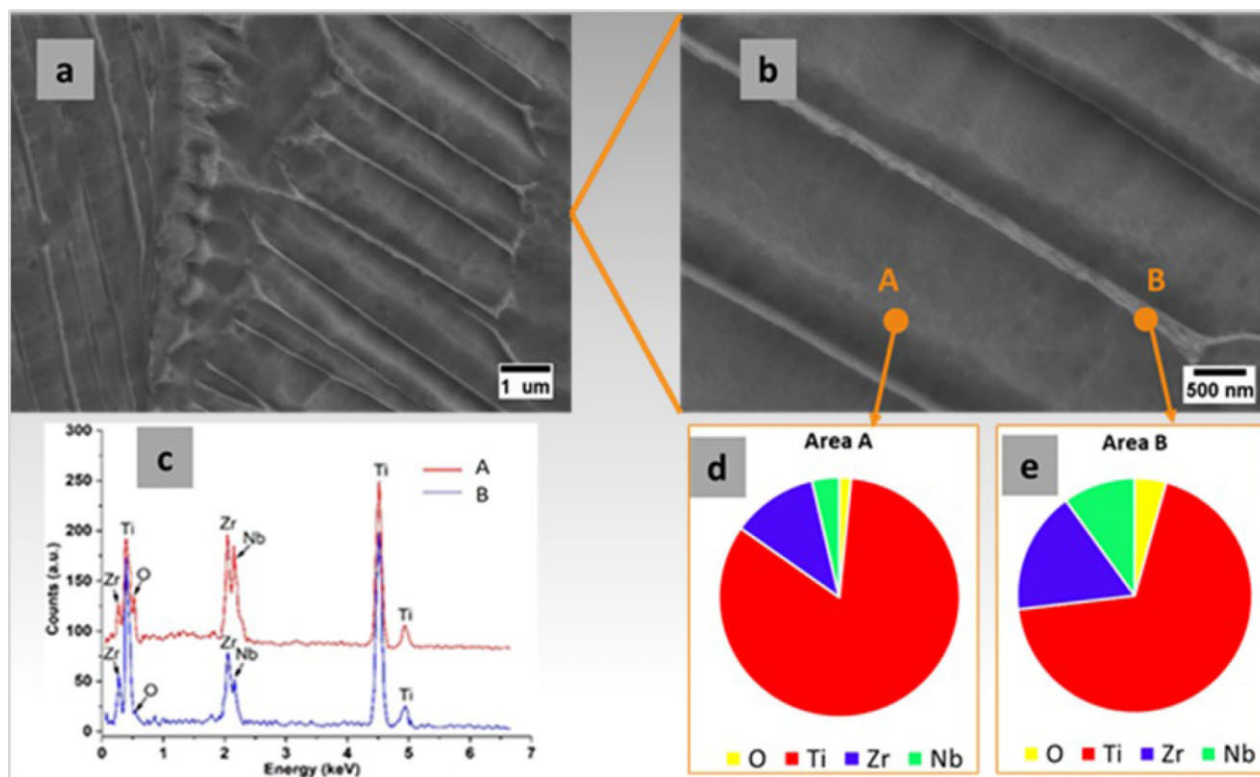


Fig. 1. SEM microstructure: a) close to the grain boundary; b) at higher magnification; c) EDS spectra; d) elemental quantification at Area A; e) elemental quantification at Area B.

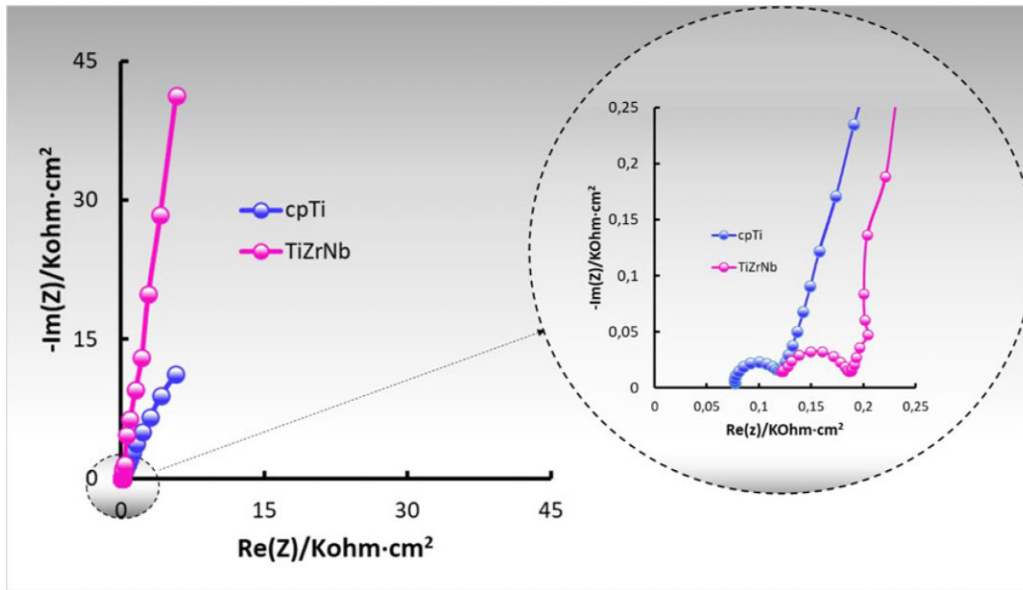


Fig. 2. Nyquist diagrams of Ti - cp and Ti-15Zr-5Nb tested in acid solution.

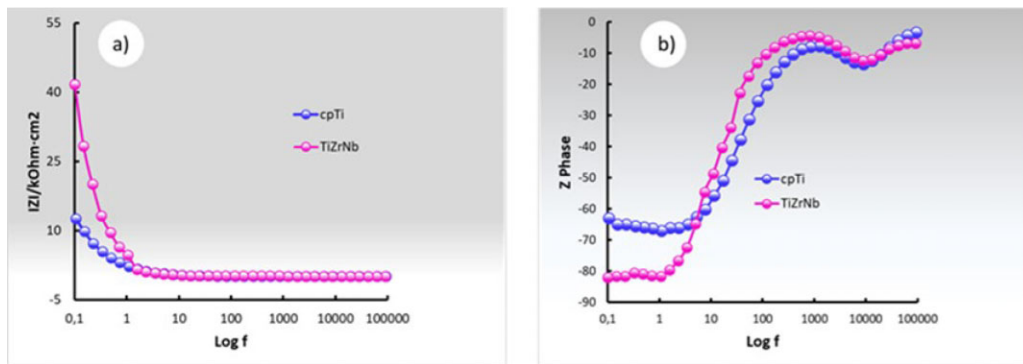


Fig. 3. Bode diagrams of Ti - cp and Ti-15Zr-5Nb tested in acid solution: a) Bode-|Z|; b) Bode-phase.

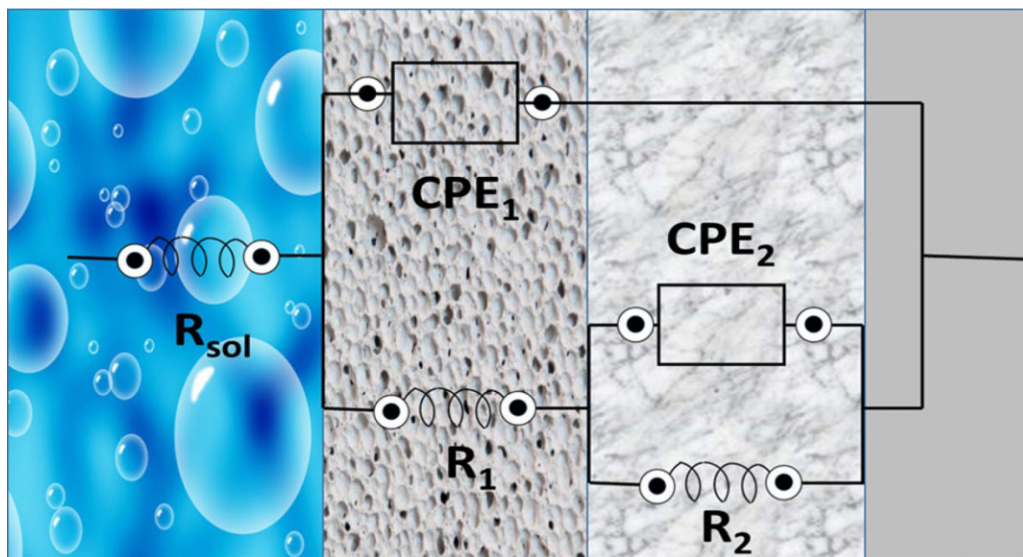


Fig. 4. Electrical equivalent circuit used for data fitting.

References

1. N. Eliaz, *Materials*, vol. 12 (2019), doi: [10.3390/ma12030407](https://doi.org/10.3390/ma12030407).
2. Vasilescu, E. *et al.*, *Werkstoffe und Korrosion* 51, (2000) 413. [https://doi.org/10.1002/1521-4176\(200006\)51:6<413::AID-MACO413>3.0.CO;2-3](https://doi.org/10.1002/1521-4176(200006)51:6<413::AID-MACO413>3.0.CO;2-3).
3. Popa, M. V. *et al.*, *Mater. Corros.* 53 (2002), [https://doi.org/10.1002/1521-4176\(200201\)53:1<51::AID-MACO51>3.0.CO;2-6](https://doi.org/10.1002/1521-4176(200201)53:1<51::AID-MACO51>3.0.CO;2-6).
4. I. Cvijović-Alagić *et al.*, *Corros. Sci.*, 53 (2011), p.796, doi: [10.1016/j.corsci.2010.11.014](https://doi.org/10.1016/j.corsci.2010.11.014).
5. A. Shi *et al.*, *Mater. Sci. Eng. C*, 126 (2021), doi: [10.1016/j.msec.2021.112116](https://doi.org/10.1016/j.msec.2021.112116).
6. J. M. Calderon Moreno *et al.*, *Mater. Corros.* 65 (2014) p.703, doi: [10.1002/maco.201307053](https://doi.org/10.1002/maco.201307053).
7. Jimenez-Marcos, C., *et al.*, *Bioengineering*, 9(2022), 686, <https://doi.org/10.3390/bioengineering9110686>
8. B.A. Boukamp, *Solid State Ionics*, 20 (1986) p.31, [https://doi.org/10.1016/0167-2738\(86\)90031-7](https://doi.org/10.1016/0167-2738(86)90031-7).